Scaling laws in annealed LiCoO x films

M. U. Kleinke, J. Davalos, C. Polo da Fonseca, and A. Gorenstein

Citation: Applied Physics Letters **74**, 1683 (1999); doi: 10.1063/1.123654
View online: http://dx.doi.org/10.1063/1.123654
View Table of Contents: http://scitation.aip.org/content/aip/journal/apl/74/12?ver=pdfcov
Published by the AIP Publishing

Scaling laws in annealed $LiCoO_x$ films

M. U. Kleinke,[a] J. Davalos C. Polo da Fonseca, and A. Gorenstein
DFA/IFGW/UNICAMP, CP 6165, CEP 13081-970, Campinas, SP, Brazil

(Received 16 November 1998; accepted for publication 26 January 1999)

The surface morphology evolution due to the annealing process of $LiCoO_x$ thin films deposited by rf sputtering is studied by means of an atomic force microscope. Linear relationships were observed in log–log plots of interface width versus window length, as predicted by scaling laws. For as-grown films, only one growth exponent α is evidenced. For annealed films two different slopes α_1 and α_2 were observed, indicating distinct growth dynamics in the system. The roughness exponent for the as-grown film and the internal morphology of the crystalline grains for the annealed films can be described by a diffusional process. The macrostructure shows characteristics of a Kardar–Parisi–Zhang system [M. Kardar, G. Parisi, Y. C. Zhang, Phys. Rev. Lett. **56**, 889 (1986); J. Krim and G. Palasantzas, Int. J. Mod. Phys. B **9**, 599 (1995)]. An activation energy $E_d=(0.11 \pm 0.01)$ eV is determined for the diffusion process. © *1999 American Institute of Physics.* [S0003-6951(99)02212-3]

Thin-film $LiCoO_2$ (Ref. 1) can be used as cathodes in solid-state microbatteries.[2] The electrochemical charge/discharge process is a simultaneous Li^+/e^- intercalation to/from the material structure. The electrons are inserted from the substrate and the ions from the film/electrolyte interface. High battery capacities mean high intercalation levels, and are strongly dependent on the morphology of the film surface.

The most important parameter to characterize a surface is the roughness. In the last decade, the concept of fractal geometry was adopted to characterize the surface morphology. The increase in scanning probe microscope (SPM) technology and theoretical developments in the area of scaling laws applied to surface growth promoted numerous works on fractal characterization of surfaces.[3]

The fractality of a surface is determined by the surface growth dynamics. Theoretical predictions for scaling growth exponents[4] were developed for distinct surface growth processes, as the linear diffusive model[5] or the nonlinear Kardar–Parisi–Zhang (KPZ) model.[6,7]

The interface width (or roughness) of a window of area $L_w \times L_w$ over the surface is defined as

$$w^2(L_w,t)=\langle[h(x,y,t)-\overline{h}(t)]^2\rangle, \tag{1}$$

where $h(x,y,t)$ is the height value at a position (x,y) and $\overline{h}(t)$ is the height mean value. The interface width and the window length can be related by a scaling law:

$$w(L_w,t)\approx L_w^{\alpha}, \tag{2}$$

where α is the growth exponent.

Simulations for $(2+1)$ surface growth reveal an α exponent equal to 0.385 and 1.0, for the KPZ and the diffusional model, respectively.[8]

In this work, $LiCoO_x$ were deposited by rf sputtering, and submitted to a postdeposition annealing process. The dynamics of the evolution of the surface morphology due to the annealing process is studied.

The films were prepared by the technique of reactive rf sputtering, in an O_2+Ar atmosphere, as described elsewhere.[9] The (unheated) substrates were metallic Ni. The thickness of the films was 0.2 μm, as measured by profilometry. Films were annealed up to 700 °C in air.

X-ray diffraction (XRD) measurements indicated that the as-grown films are amorphous. Annealing temperatures higher than 300 °C promote crystallization of the films, evidenced in the diffractograms by the presence of the (003) and (101) $LiCoO_2$ lines and two other diffraction peaks, tentatively attributed to the (400) and (440) $Li_{1.47}Co_3O_4$ diffraction lines.

The images were obtained with a Topometrix TS2000 SPM, in the atomic force microscope (AFM) mode. Tips of high aspect ratio (Microlever tip, angle near 20°, from Park Scientific Instruments) were used, in order to minimize convolution effects. All images (300×300 pixels) were acquired with a frequency equal to 2 Hz. The scan length was varied from 200 nm to 7 μm. The topographic image data were analyzed by means of a posttreatment program based both on a multiple-image variography,[3] and a single-image variography.[10,11] The mean-interface widths were estimated over nonoverlapping windows covering the original micrographs.

Figure 1 shows a series of AFM images of as-grown films and films annealed at 300, 500, or 700 °C. Peak distances, considered as representative values of grain size, and grain angles, with respect to the mean-surface level, were estimated from height profiles, obtained from the cross section in the scanning direction. The results are presented in Table I. The as-grown film [Fig. 1(a)] reveals a series of islands, with a characteristic diameter around 100 nm; and a small peak angle (~2°), characterizing a flat smooth surface for the amorphous film. After 2 h of annealing at 300 °C, an island fracturing process starts [Fig. 1(b)]. The result is a

[a]Electronic mail: kleinke@ifi.unicamp.br

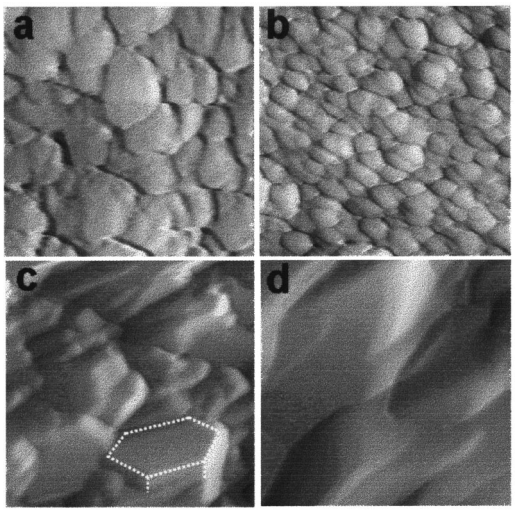

FIG. 1. AFM images of as-grown and annealed films. The scale was $0.5\,\mu\text{m}\times 0.5\,\mu\text{m}$. (a) as-grown film, micrograph height $z=47$ nm; (b) annealed at 300 °C, $z=35$ nm; (c) annealed at 500 °C, $z=178$ nm; and (d) annealed at 700 °C, $z=158$ nm.

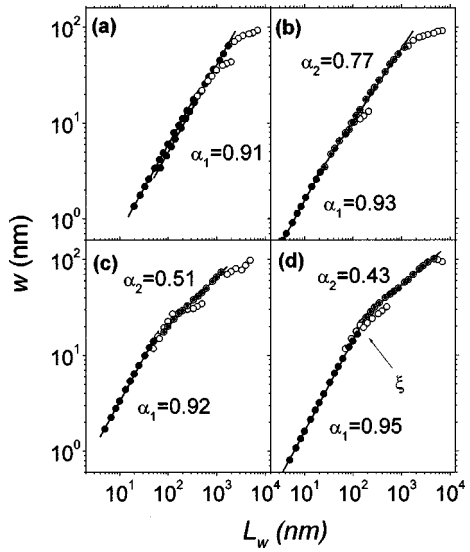

FIG. 2. Variograms of interface width vs window length. (a) as-grown film; (b) annealed at 300 °C; (c) annealed at 500 °C; and (d) annealed at 700 °C. The crossover length value ξ is indicated in (d).

cauliflower-like structure. The mean-grain size is around six times lower than before annealing. The peak angle increases from 2° [as-grown film, Fig. 1(a)] to 10° [$T_{\text{ann}}=300\,^{\circ}\text{C}$, Fig. 1(b)], indicating an asperity rise. The film annealed at $T_{\text{ann}}=500\,^{\circ}\text{C}$ exhibits sharp terraces and edges. Crystalline grains are clearly seen in the micrographs, as the hexagonal grain is evidenced in Fig. 1(c). These results are in accordance with the XRD results for films annealed at this temperature. The peak angle increases from 10° to 24°. Figure 1(d) shows the morphology of the surface annealed at 700 °C. The micrograph [Fig. 1(d)] and the corresponding topographic line manifest a clear increase in the height and length of the crystalline grains over the surface (Table I). The increase in the peak distance with T_{ann} and the XRD results are clear evidences of a transition from amorphous to crystalline structures with the appearance of crystalline grains, with well-defined terraces in the surface structure.

Figure 2 shows the $w(L_w,t)$ vs L_w log–log plots, for as-grown and annealed films at distinct temperatures. Linear relationships can be observed, as predicted by the scaling law in Eq. (2). The growth exponent α is evaluated from the slope of these linear regions. The as-grown film [Fig. 2(a)] presents only one linear region, before the width saturation value, when $w(L_w,t\rightarrow\infty)$ attain a steady state. For annealed films [Figs. 2(b), 2(c), and 2(d)], two different slopes are clearly seen, corresponding to two distinct α_1 and α_2 values, for low and high window sizes, respectively. Figure 3 summarizes these results. The growth exponent α_1 is nearly constant, with values in the range 0.91–0.95. α_2 decreases from 0.77 to 0.43, when the annealing temperature rises from ambient to 700 °C. The presence of two distinct slopes in the interface width variogram plots [Figs. 2(b), 2(c), and 2(d)] indicates distinct growth dynamics in the system. The growth process of single-crystalline grains is characterized by α_1, and is dominated by short-range correlation. The predicted value for the growth exponent in the diffusional model is 1.0[7]. This value is very close to the one calculated for the as-grown film, and for the α_1 growth exponent in annealed films. These results indicate that the growth dynamics for the sputtered as-grown film and for the crystalline grains can be described by a diffusional process. The macrostructure, observed in larger length value images, presents various preferential growth planes. These grain distribution dynamics are characterized by α_2, and present long-range correlation. The characteristic of a KPZ system is the presence of nonlinear preferential growth directions; in fact, the roughness exponent value ($\alpha_2=0.43\pm0.02$) measured at 700 °C approaches the predicted value for the growth exponent in the KPZ model[6] ($\alpha\sim0.39$).

The transition between the linear (diffusional) and nonlinear process can be characterized by a crossover length ξ, obtained from the intersection of the linear fitting of experimental data with two distinct α slopes [see Fig. 2(d)]. This

TABLE I. Peak distances and angles estimated from topographic lines.

Annealing temperature (°C)	Peak spacing (nm)	Peak angle (degree)
RT	(100±30)	(2.5±0.5)
300	(14±5)	(10±4)
500	(130±40)	(24±7)
700	(180±10)	(16.5±0.5)

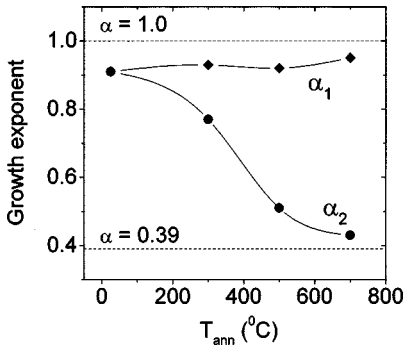

FIG. 3. Growth exponent α_1 and α_2 as a function of annealing temperature. Values predicted by the diffusional model and the KPZ model are also indicated in the figure.

crossover defines a correlation length parallel to the surface. ξ is proportional to the effective radius of the crystalline domain, and is equal to 23, 48, and 189 nm for data presented in Figs. 2(b), 2(c), and 2(d), respectively. The correlation length increases with the annealing temperature. The activation energy associated with the amorphous-crystalline transition, estimated from the $w(\xi)$ Arrhenius plot, is $E_d = (0.11 \pm 0.01)$ eV. This value is close to the one obtained by Biscarini *et al.*[12] $[E_d = (0.13 \pm 0.02)$ eV$]$ for an organic film deposited at distinct substrate temperatures. For ultrathin carbon films, $E_d = 0.12$ eV for the intrinsic surface diffusion.[13] Walton, Rhodin, and Rollins[14] estimated a value of $E_d = 0.2$ eV, for silver deposition over cleaved rock salt.

In conclusion, the surface morphology evolution due to the $LiCoO_x$ film annealing process was studied by means of atomic force microscopy. The system presents a clear transition from amorphous to crystalline structures. The roughness exponent for the as-grown film and the internal morphology of the crystalline grains can be described by a diffusional process. The macrostructure shows characteristics of a KPZ system. The transition between the two dynamics is characterized by a correlation length related to the effective radius of the crystalline domain, which increases with the annealing temperature. An activation energy associated with crystalline grain growth by the diffusional process ($E_d = 0.11 \pm 0.01$) is determined.

The authors would like to thank O. Teschke for providing access to the Topometrix TS2000 SPM, M. C. A. Fantini for the x-ray diffraction measurements and M. A. Cotta for useful discussions. Two of the authors (J.D. and C.P.d.F.) acknowledge FAPESP for a postdoctoral fellowship. Financial support was provided by FAPESP, CNPq, and FINEP.

[1] J. B. Bates, G. R. Gruzalski, N. J. Dudney, C. F. Luck, and X. Yu, Solid State Ionics **70/71**, 619 (1994).
[2] C. Julien and G. A. Nazri, *Solid-State Batteries* (Kluwer, Dordrecht, 1994).
[3] J. M. Williams and T. P. Beebe, Jr., J. Phys. Chem. **97**, 6249 (1993); **97**, 6255 (1993).
[4] F. Family, Physica A **168**, 561 (1990).
[5] S. F. Edwards and D. R. Wilkinson, Proc. R. Soc. London, Ser. A **381**, 17 (1982); D. Wolf and J. Villain, Europhys. Lett. **13**, 389 (1990).
[6] M. Kardar, G. Parisi, and Y. C. Zhang, Phys. Rev. Lett. **56**, 889 (1986).
[7] J. Krim and G. Palasantzas, Int. J. Mod. Phys. B **9**, 599 (1995).
[8] T. Halpin-Healy and Y-C. Zhang, Phys. Rep. **254**, 215 (1995).
[9] C. N. Polo da Fonseca, J. Davalos, M. Kleinke, M. C. A. Fantini, and A. Gorenstein, J. Power Sources (in press).
[10] M. V. H. Rao, B. K. Mathur, and K. L. Chopra, Appl. Phys. Lett. **65**, 124 (1994).
[11] A.-L. Barabási and H. E. Stanley, *Fractal Concepts in Surface Growth* (Cambridge University Press, Cambridge, 1995), p. 302.
[12] F. Biscarini, P. Samorí, O. Greco, and R. Zamboni, Phys. Rev. Lett. **78**, 2389 (1997).
[13] H.-A. Durand, K. Sekine, K. Etoh, K. Ito, and I. Kataoka, J. Appl. Phys. **84**, 2591 (1998).
[14] D. Whalton, T. Rhodin, and R. W. Rollins, J. Chem. Phys. **38**, 2698 (1963).